

# CHALLENGES IN DEVELOPMENT AND OPERATION OF MEMS MICROBIAL FUEL CELLS

A. Fraiwan<sup>1</sup>, S. Sundermier<sup>1</sup>, D. Han<sup>2</sup>, A. Steckl<sup>2</sup>, D.J. Hassett<sup>3</sup>, and S. Choi<sup>1\*</sup>

<sup>1</sup>Department of Electrical and Computer Engineering, SUNY Binghamton, New York, USA

<sup>2</sup>School of Electronic and Computing Systems, University of Cincinnati, USA

<sup>3</sup>Department of Molecular Genetics, Biochemistry & Microbiology, University of Cincinnati, USA

**Abstract:** Driven by increasing concerns over the energy-climate crisis and environment pollution, microbial fuel cells (MFCs) have been a major focus for renewable energy production. With the successful validation of conceptual macro-sized MFCs as a low-cost renewable energy technology, recent research has focused on miniaturizing MFCs for powering small portable electronics. However, existing micro-sized MEMS MFCs are generally limited by their relatively low power density due to the lack of fundamental knowledge and information on MEMS MFCs. In this paper, we identified the main limiting factors in developing and operating MEMS MFCs and provided suggestions to more effectively improve their performance.

**Keywords:** MEMS Microbial Fuel Cells, Micro-sized, Power Density, Limiting Factors

## INTRODUCTION

Microbial fuel cells (MFCs) are rapidly gaining acceptance as an alternative green energy technology of the future as they generate sustainable electric power from biodegradable organic compounds through microbial metabolism. Recent research has focused on miniaturizing MFCs for use in powering small portable electronics [1, 2]. However, existing micro-sized MFCs are generally limited by their relatively low power density rendering them insufficient for practical applications [3, 4]. Their power density is ~ five orders of magnitude lower than that of macro-sized MFCs, ranging from power densities of only 0.0023 to 0.4  $\mu\text{W}/\text{cm}^2$  [4]. Recently, Choi et al. reported that an (1) oxygen impermeable interface and (2) anode chamber depth were the significant limiting factors in designing MEMS MFCs [4, 5]. This is because (1) bacteria tend to consume oxygen without transferring electrons to the anode and (2) the space constraint with shallow anode chamber depth can limit the thickness of the biofilm, decreasing current generation. They achieved high power density micro-sized MFCs by optimizing the anode chamber depth and minimizing oxygen invasion into the anode chamber [5, 6]. The maximum power density of their MFC was 95  $\mu\text{W}/\text{cm}^2$ , the highest value among previously reported micro-sized MFCs and even comparable to that of macro-scale counterparts. Despite these impressive figures, the performance of micro-sized MFCs still remains insufficient to realize the prevailing potential applications, and therefore no MEMS MFCs exist to date that can independently power actual electronic devices. Thus, there is an urgent need to significantly improve the performance of the MEMS MFCs through fundamental research that can inherently maximize their power generating

capabilities. Choi et al. reported that (1) the anode energy loss is the main energy bottleneck in the MEMS MFC, causing high internal resistance and (2) the anode energy loss can be due to the poor interactions between bacteria and the gold material employed as an anode [4]. Many MEMS MFCs used gold as an electrode material, since gold is biocompatible, highly conductive, and is compatible with conventional microfabrication methods. However, their results with *Geobacter sp.* and other studies with *Shewanella sp.* suggested that bare gold is a poor electrode material for the anode of MFCs because gold does not contain functional groups, such as quinones, a natural electron acceptor for anaerobic respiration [4, 7, 8]. If one can find alternative electrode materials meeting MEMS process requirements and providing better surface characteristics for bacterial biofilm formation, the power density of MEMS MFC will increase substantially [2, 4].

Here we tested several potential anode materials in terms of current densities and proposed an alternative anode material. We also included two carbon-based anodes for the test despite their non-MEMS compatibility. This was because the best electrodes used in macro-sized MFCs have been carbon-based materials and their internal resistance has been three orders of magnitude lower than that of the MFC using the gold anode.

We also studied the effects of the significant operating parameters on the current density as the MFC size is reduced to the micro scale. Three operating parameters were examined; (1) flow rates of anolyte and catholyte, (2) external resistors for biofilm formation and (3) the role of potential bubbles in the micro-channels.

## EXPERIMENTAL DESIGN

### Operating principle

The principles of operation and electro-chemical processes inside a MFC are illustrated in Fig. 1. The basic structure of a MFC consists of two chambers the cathode and the anode separated by a proton exchange membrane (PEM). The bacteria in the anode chamber will oxidize the biomass releasing electrons as well as other chemical byproducts. The electrons are then transferred to the cathode through an external load.

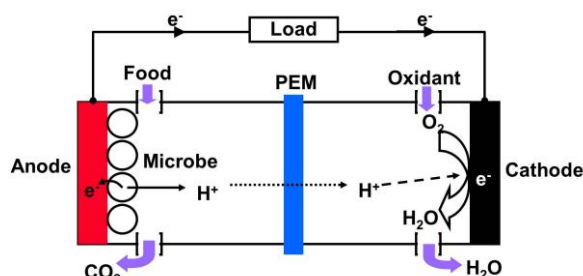


Figure 1. Principles of operation of a simplified MFC

### Inoculum

Wild-type *Shewanella oneidensis* was grown in L-broth medium as the anolyte and a phosphate-buffered ferricyanide (50 mM, pH 7.0) was used as the catholyte. Anolyte and catholyte solutions were continuously supplied using a syringe pump at a rate  $1.0 \mu\text{L min}^{-1}$  and the MFC was operated at  $30^\circ\text{C}$ .

### Device Assembly

Our MFC contains vertically stacked 50  $\mu\text{L}$  anode and cathode chambers separated by a proton exchange membrane (PEM). Each layer except for the PEM was micro-patterned by using laser micromachining and was precisely aligned. Each chamber volume was defined by a 500  $\mu\text{m}$ -thick patterned gasket. The exposed anode area/cathode per cell was  $100 \text{ mm}^2$ . Fig. 2 shows the schematic diagram of the MFC used in these studies. Photo-images of the fully assembled MFC and the individual layers are shown in Fig. 3a and Fig. 3b, respectively. Four MEMS MFCs were prepared with different anode materials; gold (sputtered), gold-coated nano-fiber, carbon paper (Fuel Cell Store,  $0.48 \text{ g/cc}$ ,  $0.2 \text{ mm}$ ), and carbon cloth (Fuel Cell Store,  $1.75 \text{ g/cc}$ ,  $0.38 \text{ mm}$ ).

Nano-fibers were prepared by electrospinning, a versatile technique to produce nanofiber membrane because of its excellent dimensional controllability, highly porous non-woven structure and extremely high surface to volume ratio. This leads to increased interaction with bacteria and, therefore, increased current density of MFCs.

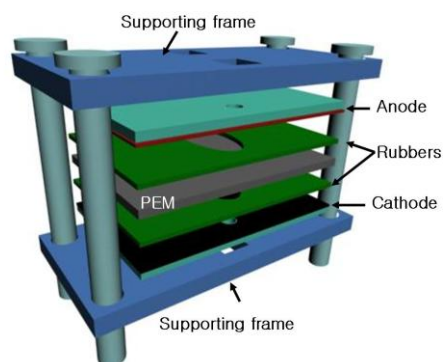


Figure 2. Schematic of the MFC-based biosensor

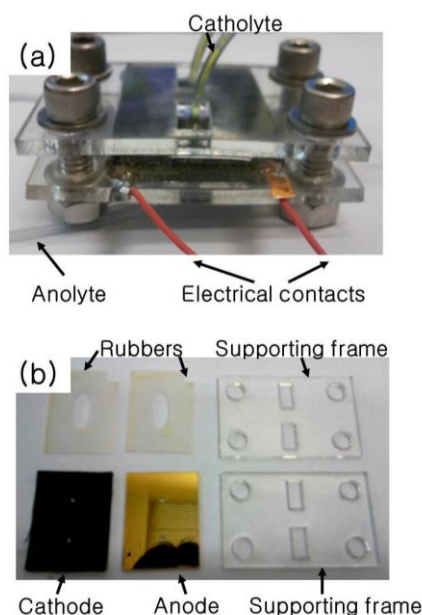


Figure 3. (a) Fully assembled MEMS MFC and (b) individual layers of the MFC

We have used poly( $\epsilon$ -caprolactone) (PCL) (Sigma-Aldrich, M.W.=90KDa) as a fiber material. The polymer solution dissolving 10wt% of PCL in 2,2,2-Trifluoroethanol (TFE) (Acros Organics, 99.8% purity) solvent was constantly fed at  $1.2 \text{ mL/hr}$  by a syringe pump. High voltage  $\sim 12 \text{ KV}$  was applied across a gap of 20cm between the needle and the collector. Resulting electrospun PCL fibers have a diameter of  $\sim 1.1 \mu\text{m}$ , with a standard deviation of  $\sim 0.3 \mu\text{m}$ . After the electrospinning process, the Denton mini-sputter system is utilized to sputter gold on electrospun fiber membranes for 10 min. No noticeable change in fiber diameter and membrane porosity was observed for the gold-coated PCL nanofibers. Interestingly, the gold coated PCL fiber membranes provide very low resistivity of  $\sim 7 \times 10^{-3} \Omega \cdot \text{cm}$ , even though the sputtered gold does not fully cover the shadowed portion of the fibers.

## Measurement Setup

The test design we used to monitor the performance of the MEMS MFC is shown in Fig. 4. We measured the potential between the anode and the cathode by a data acquisition system (National Instrument, USB-6212) and recorded the results every 1 min via a customized LabVIEW interface. An external resistor, connected between the electrodes of the MFC, closed the circuit. The current through the load resistor was calculated using Ohm's law.

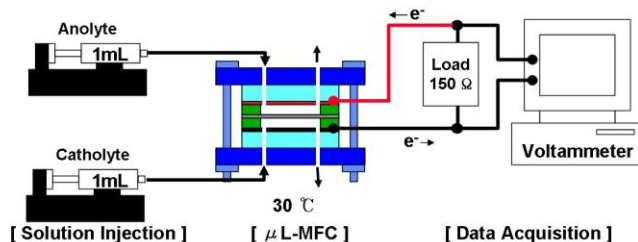


Figure 4. Schematic of test setup for monitoring the MEMS MFC.

## RESULTS AND DISCUSSION

### Anode materials for MEMS MFCs

The current densities from four anode materials in MEMS MFC were compared; (1) gold, (2) gold-coated nano-fiber, (3) carbon paper and (4) carbon cloth. The maximum current generated by the gold anode was only about  $2 \mu\text{A}/\text{cm}^2$  while the carbon cloth and carbon paper produced much higher current densities,  $13 \mu\text{A}/\text{cm}^2$  and  $4 \mu\text{A}/\text{cm}^2$ , respectively. This result is in good agreement with the previous results [4, 8]. However, carbon-based materials are not suitable for MEMS MFCs because they are not compatible with necessary microfabrication processes. As an alternative candidate, we tested gold-coated nano-fiber anode with high surface area, generating approximately two times more current density than the bare-gold MFCs.

### Flow rates

We also measured the current densities for the different flow rates of the anolyte and catholyte; 2, 5, 20, and  $100 \mu\text{L}/\text{min}$ . (Fig. 6). The current density was independent of flow rate in the anode compartment while the current densities increased with a more rapid flow rate of catholyte. This result suggests that the MEMS MFCs do not suffer from the mass transfer loss of anolyte to provide more organic food to the bacteria. Rather, the concentration loss of catholyte and/or  $\text{O}_2$  is a more dominant factor in the performance of MEMS MFCs.

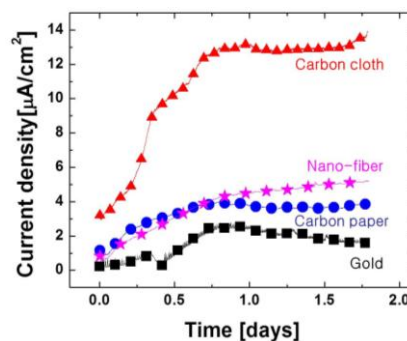
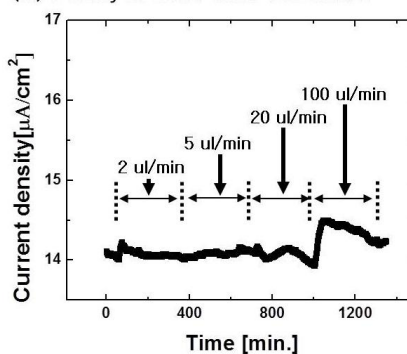


Figure 5. Currents produced from four MFCs, in which different anode materials are used.

### (a) Anolyte flow rate variation



### (b) Catholyte flow rate variation

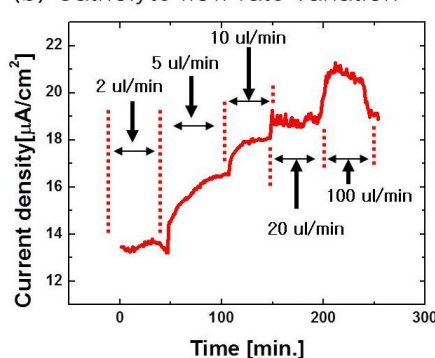


Figure 6. Effects of the flow rates of (a) anolyte and (b) catholyte on the current density of the MFC

### Biofilm formation

In addition, we examined the effect of the external load on the biofilm formation in MEMS MFCs (Fig. 7). The current densities from two MEMS MFCs with different resistance ( $150 \Omega$  &  $1 \text{ k}\Omega$ ) were individually measured during biofilm formation. Each MFC generated  $1.5$  and  $13 \mu\text{A}/\text{cm}^2$ , respectively. Low external resistance ( $150 \Omega$ ) reduced the capacity for the MEMS MFC for forming the biofilm with the reverse potential between anode and cathode while high external resistor ( $1 \text{ k}\Omega$ ) allowed gradual biofilm formation throughout 24 hour period (Fig. 7).

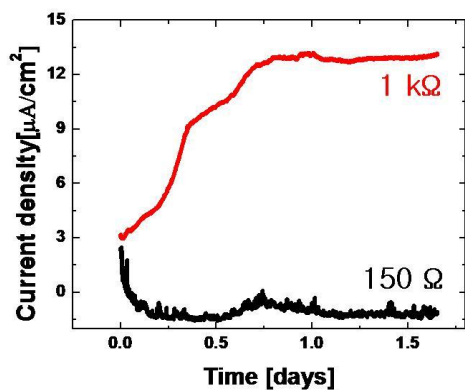


Figure 7. Effects of the external resistors on the biofilm formation of the MFC

### The “Bubble” factor

Potential bubbles may be a major limiting factor in MEMS MFCs using microfluidics. We investigated how bubble production could affect performance of the MFC. As shown in Fig. 8, it required four days to achieve maximum current density after a 12-hour bubble interruption in the anode micro-channel, while recovery was almost immediate in the cathode (Fig. 8). This indicates that bubble interruption in the anode negatively effects MFC performance.

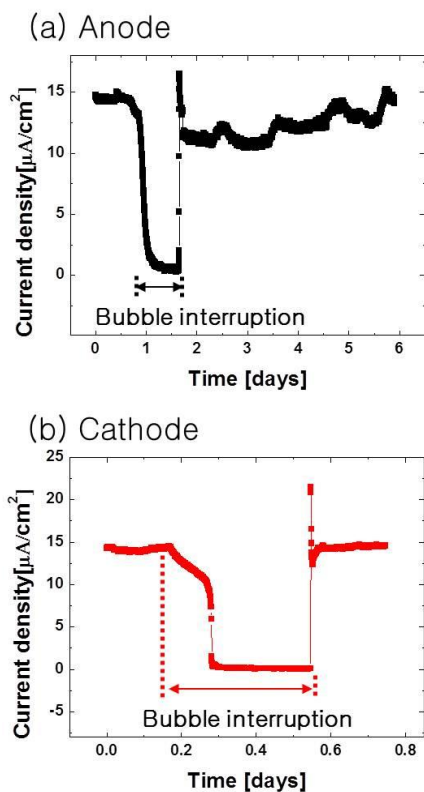


Figure 8. The role of potential bubbles in the (a) anode and (b) cathode micro-channels towards the current density of the MFC

## CONCLUSION

Here, we proposed an alternative anode material for MEMS MFCs. The gold-coated nano-fiber based MFC produced high current density even comparable to that of carbon-paper MFC. Also, we studied three operating parameters that can limit the current density produced from MEMS MFCs; flow rate of solutions, external load, and bubble invasion. For high performance of MEMS MFCs, the concentration loss for catholyte, right selection of external resistor for the optimal biofilm formation and bubble interruption in the anode chamber must all be considered.

## REFERENCES

- [1] Wang H.-W., Bernarda A., Huang C.-Y., Lee D.-J., Chang J.-S. 2010 Micro-Sized Microbial Fuel Cell: A Mini-Review *Biosecure Technology* **102** 235-243
- [2] Qian F., Morse D.E. 2011 Miniaturizing microbial fuel cells *Trends in Biotechnology* **29** 62-69
- [3] Qian F., Baum M., Gu Q., Morse D.E. 2009 A 1.5  $\mu\text{l}$  microbial fuel cell for on-chip bioelectricity generation *Lab on a Chip* **9** 3076-3081
- [4] Choi S., Lee H.-S., Yang Y., Parameswaran P., Torres C. I. 2011 A  $\mu\text{L}$ -Scale Micromachined Microbial Fuel Cell Having High Power Density *Lab on a Chip* **11** 1110-1117
- [5] Choi S., Chae J. 2012 Optimal Biofilm Formation and Power Generation in a Micro-sized Microbial Fuel Cell *Sensors and Actuators: A. Physical*, In-print
- [6] Choi S., Chai J. 2012  $\mu\text{L}$ -Scale Microbial Fuel Cell With Optimal Power Generation And Biofilm Formation *IEEE International Conference on Micro-Electro-Mechanical Systems (MEMS) (Paris, France, 29 January-3 February 2012)* 43-46
- [7] Choi S., Mukherjee S., Su S., Panmanee W., Irvin R.T., Hassett D.J. 2012 A 1.5 micro-liter microbial fuel cell array for rapid screening of exoelectrogenic bacteria Hilton Head Workshop *A Solid-State Sensors, Actuators and Microsystems Workshop (Hilton Head Island, SC, USA, 1-5 June 2012)* 169-172
- [8] Richter H., McCarthy K., Nevin K.P., Johnson J.P., Rotello V.M., Lovley D.R. 2008 Electricity generation by *Geobacter Sulfurreducens* attached to gold electrodes *Langmuir* **24** 4376-4379

### \*SUBMITTING AUTHOR

S. Choi, PH.D., Assistant Professor, Department of Electrical and Computer Engineering, SUNY Binghamton, E-mail: sechoi@binghamton.edu